POLITECNICO DI TORINO
Repository ISTITUZIONALE

Integration of a 1D model with FDS for multiscale analysis of tunnels

(Article begins on next page)

08 November 2022

Integration of a 1D model with FDS for multiscale analysis of tunnels

Jesus Mejias[1], Elisa Guelpa[1] & Vittorio Verda[1]
[1]Politecnico di Torino, Torino, Italy

ABSTRACT

Numerical simulations are used to reduce the number of tests required in a lot of scientific fields. It works in that way in the field of Fire science with the usage of CFD (Computational Fire Dynamics). Fire simulations take less time to complete as computer sciences advance. But tunnel simulations with long domains still take long times limiting the opportunities to develop applications in fields that require live time results, like risk assessment, emergency systems, etc.

A Multiscale algorithm is presented. This algorithm integrates Whitesmoke, a 1D algorithm developed to simulate fluid flow in networks, into FDS (Fire Dynamics Simulator), a 3D LES program used to simulate fire dynamics. The aim of this integration is optimizing both the calculation time and accuracy, using the fast solutions of the 1D in uniform zones and the detailed solutions of the FDS in complex areas.

The accuracy of the Multiscale is evaluated by comparing it to full 3D simulations. In this case, a tunnel of 4.8m x 4.8m and 600m of length is simulated. The flow velocities and temperature of Multiscale and FDS simulations are compared.

The Multiscale model achieves a time saving that is closely proportional to the portion of the domain calculated with the 1D sub-model. And, even when the simulation time is shorter the difference with the outputs obtained by the FDS is small in temperature, velocities and backlayering extension. The presented model is capable of reducing the time necessary to make a tunnel fire simulation without jeopardizing its results. Still, the Multiscale has some areas to improve and develop, as its boundary conditions, which should be improved further in the future.

KEYWORD: tunnel fires, multiscale, fds simulation

INTRODUCTION

A lot of scientific fields use different kinds of numerical simulations instead of tests, to reduce the number of tests or obtain faster or cheaper results. This is also the case with Fire science, where the usage of CFD (Computational Fire Dynamics) is capable of substituting a great amount of tests. Fire simulations take less time to complete as computer sciences and hardware develop. Still, simulations of long tunnels take long times limiting the opportunities to develop applications in fields that require live time results, like risk assessment, emergency systems, VR training, etc.

Fire dynamics simulations have been a topic of interest for the last decades. The research started with simpler models evolving to the 3D models that are mostly used in the actuality. The first class of models, MFIRE [2], SPRINT [3], WHITESMOKE, among others, focused on fires in 1D network systems, applicable to structures like tunnels or mines. Then zone models were developed, BRANZFIRE [5], FSSIM [6]. These models were mostly focused towards compartment fires in series of rooms in a building. From that point 3D CFD were developed, opening new possibilities to the

simulations and raising their accuracy in most of the cases.

CFD simulations have been used to simulate various fires scenarios among them confined fires [7,8], extinction modelling [9] and tunnel fires [10,11,12,13]. In the field of tunnel fires some researches have focused in [10] the smoke movement in tilted tunnels, using simulations and scale tunnels, [11] the usage FDS (Fire Dynamics Simulator) to simulate a real life fire that happened in the Hsuehshan tunnel, [12,13] the backlayering and HRR in tunnels using FDS. Still CFD remains constrained by the amount of time it takes to finish a simulation, as the simulation may last for days of weeks depending on the length of the simulated tunnel. However, this limitation is the one the Multiscale simulations tries to minimize.

Multiscale modelling is the name that receive the group of strategies to represent problems using models of different level of complexity [17]. As an example, the areas of interest can be modelled using a more complex model, like a 3D CFD, and simpler tools can be used in other regoins, like a 1D model. The objective of them is mostly to reduce the calculation time. Several articles have proposed models of this kind [14,15,16,17,18,19,20] combining a 3D CFD in the areas with complex physics, and a 1D model elsewhere. Some examples are, [14] shows an approach where FDS (CFD) and VentFire (1D) are coupled, and study then the link among them configurating it in various ways, choosing an indirect coupling approach in the end, which can be faster but has the demerit of needing time to obtain the characteristics curves of the system, to divide it in an appropriate way. In [15] the FDS is used with its HVAC function. Here the time reduction in cold simulations is analysed. In [16] the HVAC function is used together to the MPI to further reduce the time expenditure, mostly to evaluate the time saving obtained combining them; in [17,18,19,20] ANSYS Fluent is linked to the 1D tool, Whitesmoke, here the fire is simulated as a heat source, obtaining good agreement between the multiscale and 3D simulations. So far, these approaches have shown good results in the velocity and temperature fields. However, some of the actual research lacks the modelling of heat losses, or species concentration along the 1D portion of the tunnel. Whitesmoke can cover these shortcomings, and together with FDS provide an open-source solution to the multiscale simulation of tunnel fires.

FDS was selected as the CFD code in our model, as it has the great advantage that it can be modified freely (is an open source software) and that it already is widely spread in the Fire science community. This work proposes the integrations of the Whitesmoke inside the FDS code. This allows for an excellent communication between the sub-models, and an optimization of the calculation time, by calculating the uniform far field with the 1D and focusing resources in the complex near field of the fire. Other than the flow the Whitesmoke can also handle the species transport, the thermal flow, inclined tunnels and the allocation of fans and obstructions. This Multiscale model could be applied in different fields, mainly in the tunnel fire research, but also for other kinds of tunnels scenarios, like metro tunnels, mining tunnels, subaquatic tunnels, among others. Essentially it might be useful for applications were one dimension notably lengthier than the others.

MULTISCALE MODEL

General Description of the Multiscale Algorithm:
A Multiscale model is proposed on this work. This model fully couples the Whitesmoke, a 1D fluid flow software, inside the FDS. Being compiled together and ran at the same time is possible to further increase the advantages provided by Multiscale models. Also, the Whitesmoke capability to describe in a more complete way the flow helps obtaining a more detailed 1D far domain.

The type of coupling between the two sub-models is a direct coupling, characterized by both models running together. Also, they don't share any part of the domain, which is denominated a non-overlapping coupling.
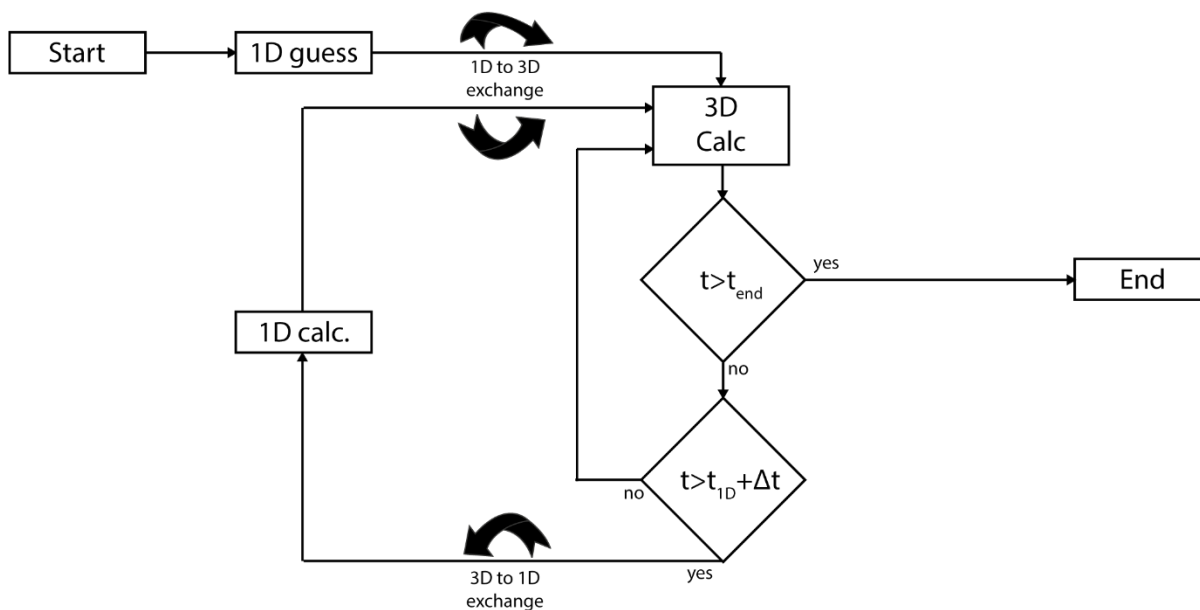
Figure 1   Multiscale Algorithm Representation

In figure 1 a scheme shows the order in which the information transfers take place in each time step. This starts with the 1D guess when the simulation starts, and then follows a loop where, every n seconds, the 3D model imposes the 1D model boundaries and vice versa.

1D description and Characteristics:

The far field of the simulation is calculated using the Whitesmoke. This model solves three groups of equations calculating the fluid dynamic flow, thermodynamic flow and mass-transport in the 1D field. These groups of equations are approached in different ways.

Network Modelling

The Graph Theory [22] is used in this part of the model. It allows for a simple representation of domains where one dimension is preponderant above the others [21]. Through the graph theory the tunnel domain is described using nodes and branches. The branches represent fractions of the tunnel, that can contain fans, obstructions, or other characteristics that have to be modelled. These branches are limited by nodes, they connect the branches between them, and impose boundary conditions towards the 3D and the exterior of the simulation. This configuration allows for the creation of a matrix that simplifies the calculations, the incidence matrix. This matrix has one row for each node and one column for each branch. The matrix marks inlets (as +1) and outlets (as -1).

Fluid Dynamics Model

The fluid dynamics of the flow are solved using a modified version of the 3D time dependent Navier-Stokes equations for continuity and momentum. Different assumptions are made to do these modifications. One dimension is assumed preponderant over the other two, considering the equations unidimensional. This change is seen from Eq. 1 to Eq. 2, for continuity, and from Eq. 3 to Eq. 4, for the momentum equation.

$$\frac{\partial \rho}{\partial t} + \nabla.(\rho u) = 0 \qquad (1)$$

$$\frac{\partial \rho}{\partial t} + \frac{\partial \rho u}{\partial x} = 0 \tag{2}$$

$$\frac{\partial \rho u}{\partial t} + \nabla.(\rho u u) = -\nabla p + \nabla.\tau + \Delta P_{source} \tag{3}$$

$$\rho \frac{\partial u}{\partial t} + \rho u \frac{\partial u}{\partial x} = -\frac{\partial p}{\partial x} - \Delta P_{fric} + \Delta P_{source} \tag{4}$$

In Eq. 4, due to the elimination of the y and z dimensions, the viscous term $\nabla.\tau$ losses most of its significance. Consequently, the viscous losses are included in the term ΔP_{fric}. The term ΔP_{source}, in Eq. 3 and Eq. 4, is a momentum source term including momentum due to fans, buoyancy, among others.

Next, the equations are redeveloped around the branches (momentum) or nodes (continuity). The backward Euler method is used as the time advancing scheme. The final shape of the equations is seen in Eq. 5, for continuity, and Eq. 6, for momentum. Must be remarked that the total pressure (P) in the Eq. 6 is the sum of the pressure, kinetic and buoyancy terms, as shown in Eq.7, subtracting the buoyancy term from the source term ΔP_{source}.

$$\frac{(\rho_i^t - \rho_i^{t-\Delta t})}{\Delta t}\left(\sum_j \frac{A_j L_j}{2}\right) + \sum_j u_j A_j \rho_j + G_{ext,i} = 0 \tag{5}$$

$$\rho_j \frac{(u_j^t - u_j^{t-\Delta t})}{\Delta t} L_j + (P_i - P_{i-1}) - \Delta P_{fric} + \Delta P_{source} = 0 \tag{6}$$

$$P_i = p_i + \frac{\rho_i u_i^2}{2} + \rho_i g z_i \tag{7}$$

In the formulas ρ stands for density [kg/m³], u for velocity [m/s], t for time [s], v for kinematic viscosity [Kg/m.s], L for Length of the branch [m], p for pressure [Pa], A for area [m²], G for flux [kg/s], g for gravity, z for height, i enumerates the nodes and j the branches. Also, G_{EXT} [kg/s] is added in Eq. 5 to consider possible sources of flow into the nodes. A complete explanation of the development of these equations is found in [17,21,23].

Thermal model

The construction of the formula to calculate the thermal field shares some steps with the construction of the fluid flow model. It starts with the transient energy equation of Navier-Stokes. This equation is then reduced to a unidimensional form, as seen in Eq. 8 and Eq. 9.

$$\frac{\partial(\rho c_p T)}{\partial t} + \nabla.(\rho c_p u T) = \nabla.k\nabla T + \varphi_v - \varphi_l \tag{8}$$

$$\rho c_p \frac{\partial T}{\partial t} + \rho c_p u \frac{\partial T}{\partial x} = k \frac{\partial^2 T}{\partial x^2} + \varphi_v - \varphi_l \tag{9}$$

Two terms are added in the right side of Eq. 9. These two terms represent the possibility of having a volumetric heat source [W/m³], φ_v, and the heat losses through the walls [W/m³], φ_l. The next step is to integrate the Eq. 9 and then discretize it in a control volume surrounding the nodes of the network. In this discretization the temperature of a branch is considered using the upwind model (affirming that the temperature of a branch is the temperature in its upstream node). Finally, the first term on the left is formulated using the Backward Euler method, as it is a time dependent term, finally arriving to the expression in equation Eq. 10.

$$\rho_i{}^t c_{pi} \frac{(T_i^t - T_i^{t-\Delta t})}{\Delta t} \Delta V + \sum_j \rho_j{}^t c_{pj} u_j{}^t A_j T_j{}^t = \sum_j k_j \frac{\partial T^t}{\partial x}\Big|_j A_j + \phi_{v,i} - \phi_{l,i} \tag{10}$$

Here c_p is the heat capacity [J/kg.K], T the temperature [°C], k the conductivity [W/m.K], ϕ_v the heat generation [W] and ϕ_l are the heat losses [W].

The $\phi_{l,i}$ term contains the heat losses in a node that is equal to the sum of the losses across the surface of the half of all the branches connected to it. In Eq. 11, Ω_j is the perimeter, U_j the global heat transfer coefficient and $T_{\infty,j}$ the temperature of the rock outside the tunnel walls. In Eq. 12 U_j is calculated using h_j, the convective heat transfer coefficient, and $R_{RR,j}$, the global thermal resistance of the rock. Finally, the convective heat transfer coefficient is defined in the Eq. 13, where f_j corresponds to the branch friction coefficient.

$$\phi_{l,i} = \sum_j \frac{L_j}{2} \Omega_j U_j \big(T_i - T_{\infty,j}\big) \tag{11}$$

$$U_j = \left(\frac{i}{h_j} + R_{RR,j}\right)^{-1} \tag{12}$$

$$h_j = \frac{1}{8} f_j c_{p,j} \frac{G_j}{A_j} \tag{13}$$

The assumptions and procedures employed to arrive to these expressions are furtherly explained in [17,21,23].

Mass transport model

This part of the model is built around an advective-diffusive expression [21]. The advective part describes the motion of the contaminants with the air. The diffusive part, obeying Fick's theory, makes the concentration proportional to the mean concentration gradient. The unidimensional representation of this equation corresponds to Eq.14.

$$\frac{\partial c}{\partial t} + u \frac{\partial c}{\partial x} = D \frac{\partial^2 c}{\partial x^2} + S_p \tag{14}$$

C is the mass concentration [kg/m³] of the species in the air, D the diffusion tensor [m²/s] and S_p represents a source term for other species [kg/m³.s]. Then integrating inside a control volume that has a node as its centre, Eq. 15 is obtained.

$$\int_{CV} \frac{\partial c}{\partial t} \partial V + \sum_j u_j{}^t A_j C_j{}^t = \sum_j D_j A_j \frac{C_i^t - C_j^t}{L_j} + S_{p,i} \tag{15}$$

The concentration coming from each branch, C_j is calculated similar to the temperatures of thermal model, using the upwind scheme. Therefore, the concentration C_j is the same concentration of the upstream node. Finally, the time dependent term is expanded using the backward Euler formulation, obtaining Eq. 16.

$$\frac{C_i^t - C_i^{t-\Delta t}}{\Delta t} + \sum_j u_j{}^t A_j C_j{}^t = \sum_j D_j A_j \frac{C_i^t - C_j^t}{L_j} + S_{p,i} \tag{16}$$

Matrix formulation

The previously mentioned incidence matrix is used to reformulate the equations. Through this procedure the obtained equations are independent of the topology of the network, as the incidence matrix synthetizes the flow directions and links of branches with nodes.

$$AG^t + G_{EXT}^t + r^t = 0 \tag{17}$$

In Eq. 17 we can observe the simplified continuity equation. As before it is evaluated in the nodes, the term AG^t accounts for the flow entering the node from linked branches (as the product of the A incidence matrix, non-dimensional, and the flow vector G [m^3/s]), G^t_{EXT} the flow entering or exiting to the exterior and r^t is accumulation time dependent term.

$$A^T \cdot P^t = (R^t + C^t) \cdot G^t - t^t - s^t \tag{18}$$

Then in Eq. 18 can be seen the relation between the pressure change (product of the transposed incidence matrix A^T and the pressure P), on the left side. And the flow losses and localized pressure variations, in the right. This losses are calculated taking into account the R, matrix of resistivity that includes the localized and distributed losses, C and s that represent a resistivity and other pressure effects due to the transient calculations, and t represents the other sources of pressure, among them fans, piston effect, buoyancy.

The matrix form of the thermal model is in Eq. 19. In Eq. 19 the left side contains a Diagonal "Mass" matrix M^t, the Stiffness matrix K^t and the Temperature vector T^t, meanwhile the right side has the f^t that corresponds to the known temperatures, as boundary conditions, $M^{(t-\Delta t)} T^{(t-t\Delta)}$ is the "mass" and temperatures of the previous time step and $\Phi_{v,i}$ is a heat source term.

$$(M^t + K^t)T^t = f^t + \Phi_{v,i} + M^{t-\Delta t}T^{t-\Delta t} \tag{19}$$

Equation 20 shows the matrixial formula for the mass transportation model. In the left side are the variables related to the change of concentration, and in the left the ones related to the known concentrations and species sources. In short, the structure is the same that the thermal model has.

$$\left(M_C{}^t + K_C{}^t\right)C^t = f_C{}^t + S_p{}^t + M_C{}^{t-\Delta t}C^{t-\Delta t} \tag{20}$$

Equation 20 has as Eq. 19 a "mass", M_c, and stiffness, K_c, matrix, a vector of known concentrations, f_c, a source term of concentration, S_p and the las term is the product of the "mass" and temperature of the previous time step.

Solution procedure

The SIMPLE algorithm (Semi-Implicit Method for Pressure Linked Equations), proposed by Patankar and Spalding [24], is used to obtain the model solution. The SIMPLE is based in a guess and correct procedure [23] that uses the matrixial form of the equations to iterate the system until finding the flow and pressures that take the system towards equilibrium, in each time step.

The simplified procedure the SIMPLE adopts is shown in fig.2. This procedure starts the update of the variables, flow and pressure, then the flow is calculated with the updated pressure, and a change of pressure is calculated with the new flow. The pressure and flow for the next time step are obtained using under-relaxation constants, α_p and α_g both equal to 0.5. Subsequently, both the temperature and concentration are updated.
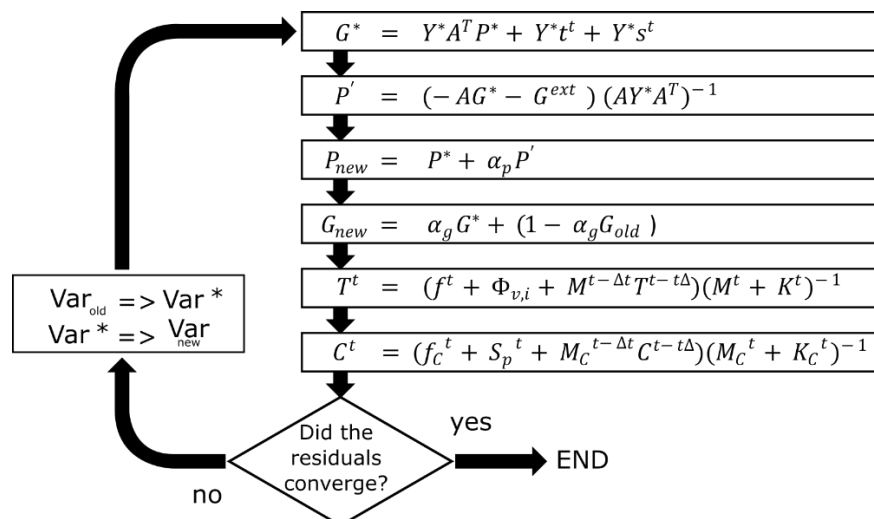
$$G^* = Y^* A^T P^* + Y^* t^t + Y^* s^t$$

$$P^{'} = (-AG^* - G^{ext})(AY^* A^T)^{-1}$$

$$P_{new} = P^* + \alpha_p P^{'}$$

$$G_{new} = \alpha_g G^* + (1 - \alpha_g G_{old})$$

$$T^t = (f^t + \Phi_{v,i} + M^{t-\Delta t} T^{t-t\Delta})(M^t + K^t)^{-1}$$

$$C^t = (f_c{}^t + S_p{}^t + M_C{}^{t-\Delta t} C^{t-t\Delta})(M_C{}^t + K_C{}^t)^{-1}$$

Var$_{old}$ => Var *
Var * => Var$_{new}$

Did the residuals converge?

yes

END

no

Figure 2 SIMPLE Algorithm Procedure

3D descriptions and characteristics

The CFD code that simulates the 3D area is the FDS, in its 6.7 version. The FDS is an open source program, its coded in Fortran 90, and is capable of simulating a wide selection of fire and ventilation scenarios. Some of the main characteristics of diverse tools of the FDS are:

•Geometry: The meshes and obstructions most have rectangular cuboid shapes, or cubical shapes for more stability. Parallelization can be implemented by using more than one mesh and using the MPI (Message Passing Interface) tool.

•Hydrodynamic Model: Implements the LES (Large Eddy Simulation) turbulence model, when not using DNS (Direct Numerical Simulation). The solution is obtained through a two-step "predictor corrector" algorithm that solves the Navier-Stokes equations.

•Combustion model: Combustion is treated in several modes, from the Arrhenius reaction formula to a simple model of mixing controlled reaction, where mixed equals burnt. The default combustion model is a single step, mixing-controlled reaction (where mixed is equal to burnt). This reaction uses only 3 reactants air, fuel and products, lumping them to make it simpler and faster.

For more details on how the FDS works we refer the reader to the different guides included with the FDS, the User Guide and the Technical Reference Guide [1,26].

Coupling between the 3D and 1D models

The coupling between the sub algorithms can be classified as a non-overlapping Dirichlet-Neumann Direct coupling, this according to [25]. This means that the meshes of the two sub-algorithms don't share any part of the domain, as non-overlapping, and that the two algorithms work together, sharing data while they run their calculations, as a direct coupling.

FDS and WhiteSmoke are compiled together, which makes possible a constant and fast communication between them. In order to achieve this, several parts of the codes were modified to allow a fast exchange of data, and to introduce the new kinds of boundary conditions needed for the interface between the sub-models. In this sense other than extracting data a new namelist was introduced to the FDS, the EXCH namelist, used to declare the position and characteristics of the boundary between the 3D and 1D.

Specifically, this new namelist can assign the boundary to kinds of profiles, with different functions, the "VEL" boundary and the "PRES" boundary condition.

"PRES" Boundary

In the "PRES" boundary the 3D imposes the pressure to the 1D and the 1D instead imposes the flow, including its temperature and composition, to the 3D. This boundary was built using as a base the VENTs in FDS, and therefore shares its properties. This means that the boundary behaves as a wall capable of allowing the flow of species in just one direction, being an inlet or outlet. Then, the exchange that occurs in this boundary assigns the average of the pressure in the wall as the pressure in the node linked to this BC. And at the same time assigns the flow, temperature and concentration, of the 1D node as uniform properties of the wall boundary.

"VEL" Boundary

Instead, in the "VEL" boundary condition happens the opposite, the 3D imposes the flow, including the temperature and composition, and the 1D imposes the pressure. Like the previous boundary was similar to the VENT, this one is similar to the OPEN boundary. Being similar to the OPEN boundary gives it the capability to have flows in both directions simultaneously. Then, regarding the data exchange now the 1D node imposes the pressure uniform pressure in the wall, using the dynamic pressure property, and the 3D imposes the average of the flow, temperature and concentration, of the cross-section, to the connecting node of the 1D.

Boundary considerations

The FDS user guide [1], recommends having one pressure and one flow boundary condition when simulating tunnels, opposed to using 2 pressure conditions. Because of this both of the proposed boundary conditions are useful. Still, they must be placed in the side of the simulation that exploits better their capabilities. Therefore, the recommended layout would involve a PRES boundary condition upstream of the fire, at a distance higher than the backlayering distance (that can be calculated with different expressions like [13]) and a "VEL" boundary condition downstream of the fire. The distance downstream of the fire before the 1D boundary is mainly defined as a compromise in accuracy and computational speed, as having a small 3D domain is faster to simulate but introduces to the 1D properties that are not uniform in the cross-section and that will not be accurately simulated in the 1D. The ideal downstream distance would let the density and temperature arrive to the environmental value, but to be reasonable it is shorten to a distance where the temperature and density gradients are relatively low. A schematic example can be seen in Fig. 3.
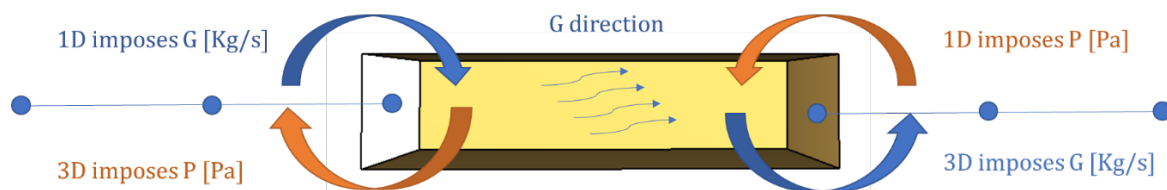

Figure 3 Boundary Placement

Differences and Improvements regarding the HVAC function of the FDS

The FDS has developed a functionality inside its code to add Heating, Ventilation and Air Conditioning systems to its simulations. The HVAC system uses a 1D representation of the ventilation network also formed of nodes and ducts, can impose ambient condition in its ends and link different closed zones inside the same simulation.

The HVAC and the 1D-3D algorithm proposed represent the networks in the same way, but the treatment that is given to the data is different. The 1D-3D calculates most of the quantities the HVAC

does, as the losses (both minor and flow losses), the mass fractions, among others. Also, it has some added capabilities like calculating the heat losses through the network, being able to impose pressurized and velocity boundaries, other than just ambient and another closed chamber. Even more, the way the 1D3D is built is bulkier, featuring a direct coupling between both algorithms, while FDS and HVAC has a non-direct coupling and may struggle with big inlets or outlets, as it was not meant for them.

TEST CASES

A one carriage tunnel was simulated with the Multiscale model and only with FDS. Comparing the results is possible appreciate the capabilities of the Multiscale.

The tunnel dimensions are of 4.8m x 4.8m x 600m. The roughness of the walls is of 0.0042m. The walls are modelled as inert walls at a fixed temperature, simulating the heat exchange was evaluated and was seen that in the present case the temperature difference was similar in both cases.

The Heat comes from a 2MW fire. The combustible is Diesel, placed in a pool, with a Heat of combustion of 43027 kJ/kg and a soot yield of 5%. The Diesel pool dimension are 1.2m x 1.2m x 0.3m and it is placed at 300 meters of the tunnel entrance, on the floor in the midpoint of the track.
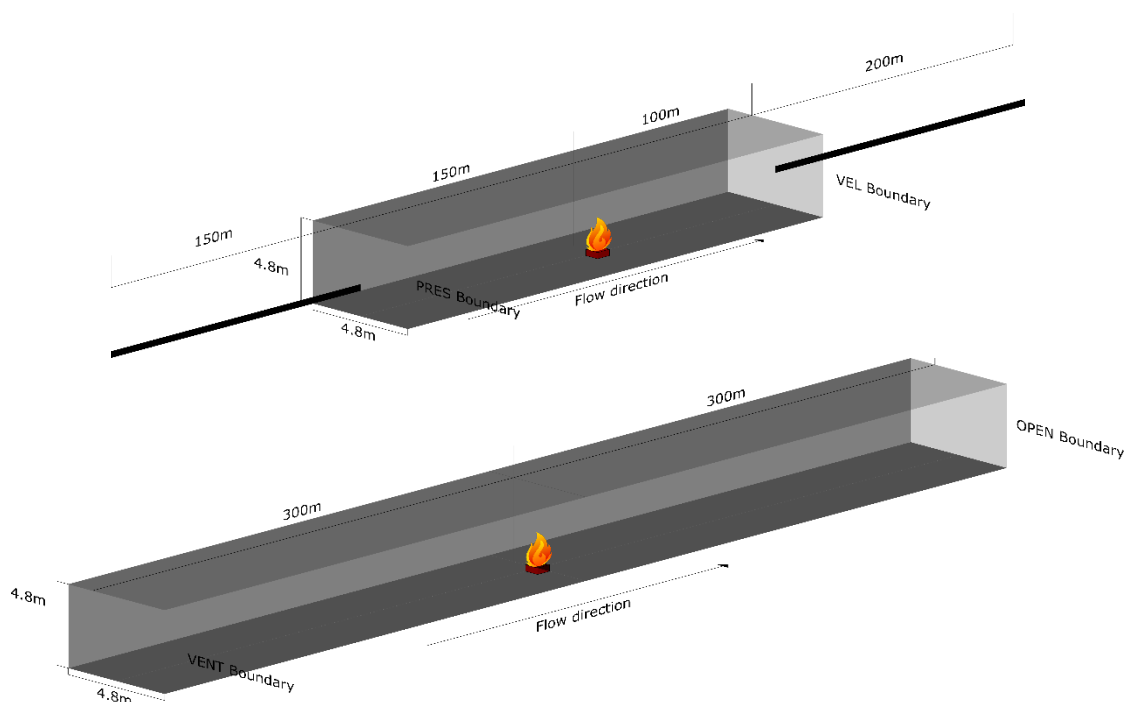

Figure 4 Multiscale (up) and Full 3D (down) simulation domains

The full FDS simulation (600m) and the Multiscale simulation (250-3D 350-1D), as they can be seen in figure 4, are compared. Both simulations are compared twice, using different mesh sizes, 0.3m and 0.25m, in their cubical meshes.

The size of the 3D domain in the Multiscale was selected considering different factors. In the upstream boundary the distance was selected to be superior to the backlayering distance, this distance was calculated using different the formulas from [4] . Meanwhile, the downstream boundary distance was selected as to provide a sufficiently uniform flow and temperature field, but being permissive. Is necessary in this case to pick a distance that ensures time reduction with not much loss of accuracy.

RESULTS

The results from the FDS and Multiscale are compared to show the usefulness of the Multiscale towards time saving and accuracy.
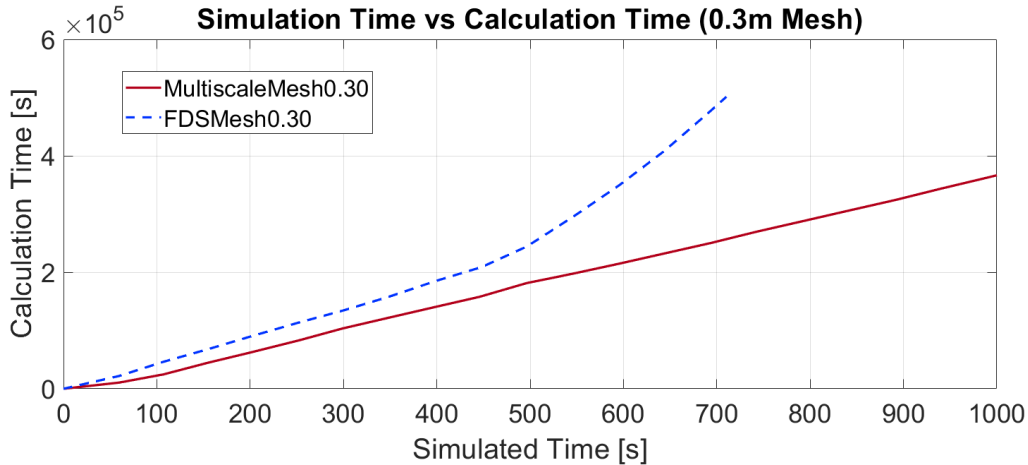

Figure 5 Calculation time comparison between a Multiscale and FDS simulation, with a mesh of 0.3m
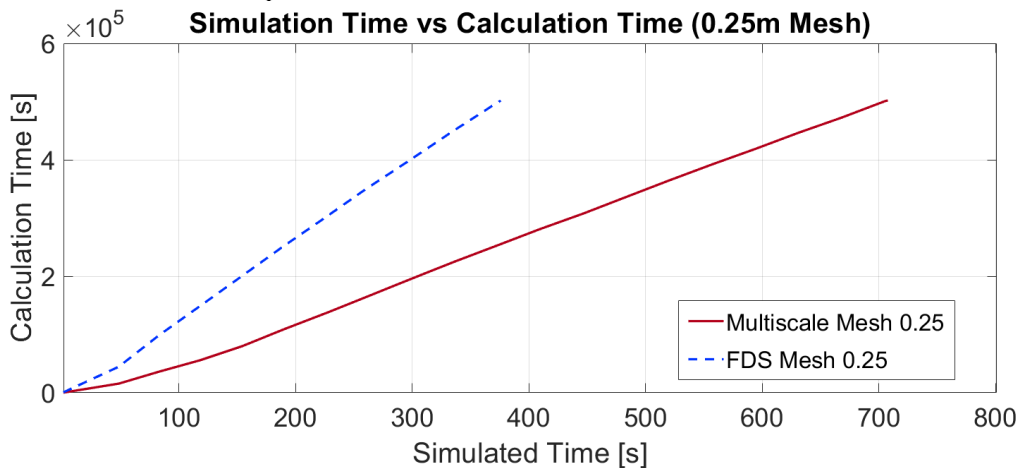

Figure 6 Calculation time comparison between a Multiscale and FDS simulation, with a mesh of 0.25m

In figure 5 and 6 the models are compared. In both graphs is appreciable that the FDS alone needs more calculation time to simulate the same amount of time. In the case of figure 6 the time the FDS needs doubles the time needed by the multiscale; This reflects a reduction of calculation time almost proportional to the domain portion simulated in 1D. In the figure 5 the difference in the first 400 seconds of the simulation is close to a 20- 30%, but it grows after this point. The cause of the growth in the FDS time is mostly due to irregularities in the exit boundary after the flow arrives to it. As the flow is hotter than the exterior the buoyancy forces push the flow upwards, producing faster velocities in this region and flow reversal in the lower part of the tunnel.

Buoyancy as a physical phenomenon is working in a correct way, but the velocity distribution it creates close to the boundary is unstable and can create issues with pressure, temperature and velocity. These issues are also reflected in figures 7 and 8.
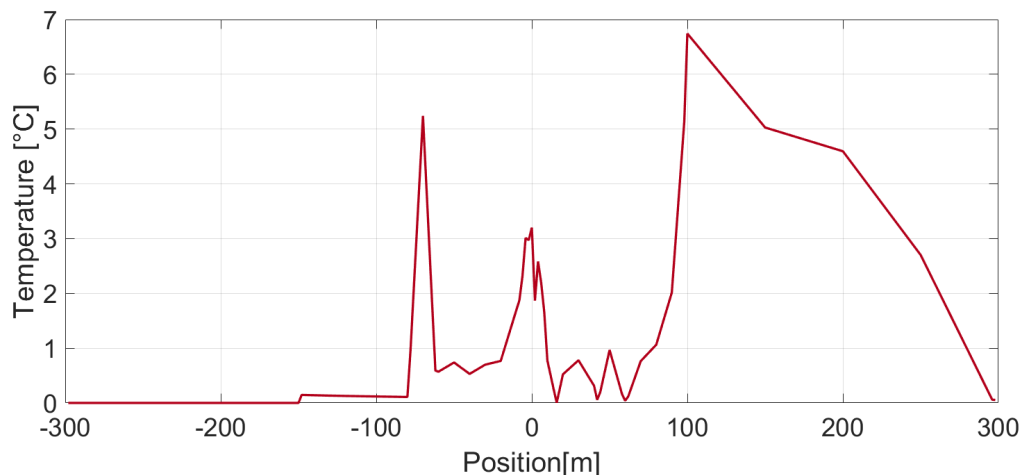
184

Figure 7 Temperature Difference between the Full 3D and Multiscale simulations with the 0.3m mesh
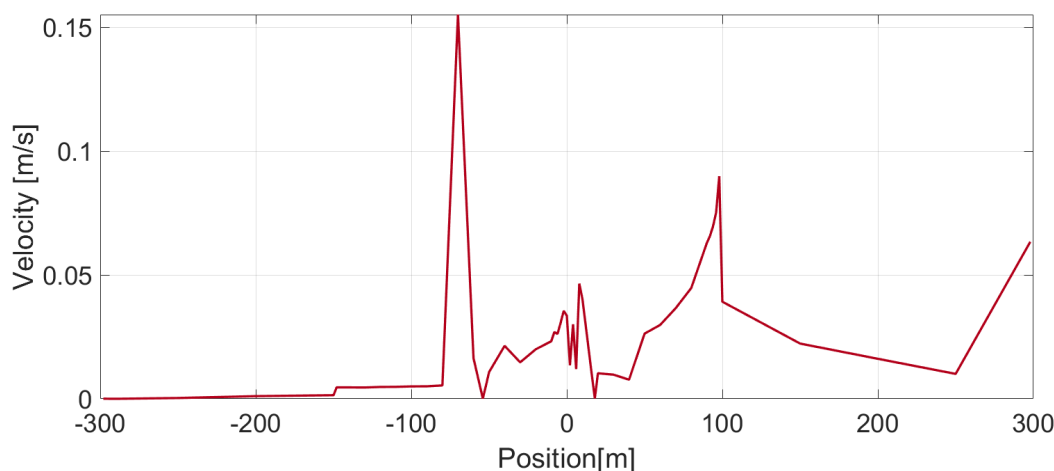

Figure 8 Velocity Difference between the Full 3D and Multiscale simulations with the 0.3m mesh

The figures 7 and 8 evidence that the results of both of the models are similar, the differences in velocity remain below the 0.15 m/s and in temperature below the 7 degrees Celsius.

In both figure 7 and 8 a total of 4 points of interest can be clearly distinguished. The first one is around 80 meters upstream of the fire. This first point matches with the backlayering lengths of both simulations. The sudden raise and decrease of the temperature and velocity difference are a consequence of a slight difference in the backlayering distance. Being the backlayering difference of around 5 meters the error disappears as soon as both simulations reach similar properties. The difference in velocity is important in this point as inside the backlayering length the flow has velocities in the 3 components, but upstream to it the velocity is mostly unidimensional, and therefore lower. The difference in temperature is caused by the smoke, which is hotter than the tunnel air upstream of the backlayering distance.

The second interest point would be the fire itself, positioned in the centre of the tunnel length. In this point the difference is linked to the high velocities and temperatures around the fire, and the random character of it.

The third interest point is the boundary condition between the 1D and 3D in the Multiscale simulation. Here the buoyancy at OPEN boundaries is seen in the Multiscale simulation. This buoyancy is

reflected as a sudden increase in the velocity of the multiscale before the boundary and a drop in the temperature because of the flow reversal, as cold air enters.

The last point of interest is the OPEN boundary 300 m downstream. In this point the issue is the same with the buoyancy, the velocity in the end of the 3D rises and the temperature decreases. Still, as the problems is seen both in the multiscale and in the 3D, the temperature in the end is the almost the same in both simulations.
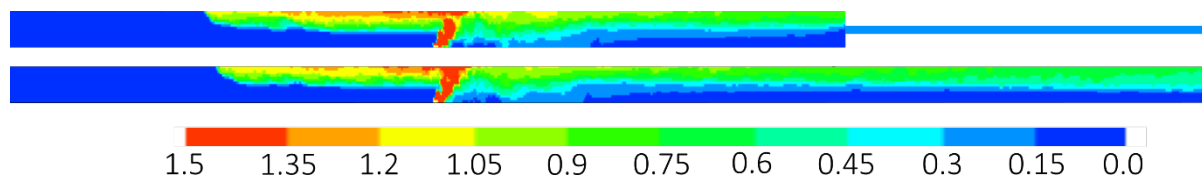

| 1.5 | 1.35 | 1.2 | 1.05 | 0.9 | 0.75 | 0.6 | 0.45 | 0.3 | 0.15 | 0.0 |

*Figure 9 Comparison of Soot mass fraction [10^{-4}*kg/kg]*

Finally, in figure 9 it is evident the light difference of the total distance occupied by the backlayering smoke. This difference develops into a velocity and temperature difference. However, both images are very similar, which supports the similarity of the simulations and the accuracy of the model as a whole.

CONCLUSION

In this paper a Multiscale Model was proposed and tested. Comparisons with a full 3D simulation indicate that it manages to save calculation time in long tunnel fire simulations without losing a considerable amount of precision. Therefore, the modification of the FDS tools, and introductions of the Whitesmoke as a 1D sub-model provides a new Multiscale tool. This development introduces new opportunities for applications of the FDS software. Still, despite the good coupling between both sub-models some imprecisions have been inherited from the OPEN boundaries.

Therefore, the development of the Multiscale model would involve further modifications in the code to obtain a more coherent boundary condition and minimize the difference between the Multiscale model simulation and the 3D simulation.

REFERENCES

1. McGrattan, K., Hostikka, S., McDermott, R., Floyd, J. and Vanella, M., *Fire Dynamics Simulator (Version 6), User's Guide*, NIST Special Publication 1019, 2013

2. Cheng, L., Ueng, T. and Liu C., Simulation of ventilation and fire in the underground facilities. *Fire Safety Journal* , **36**, 597-619, 2001

3. Riess, I., Bettelini, M. and Brandt, R., SPRINT—a design tool for fire ventilation. Proceedings of aerodynamics and ventilation of vehicle tunnels conference, Boston, USA, November 2000

4. Wu, Y. and Bakar, M., Control of smoke flow in tunnel fires using longitudinal ventilation systems—a study of the critical velocity, *Fire Safety Journal*, **35**, 363-390, 2000

5. Wade, C. and Barnett, J., A Room-Corner Fire Model Including Fire Growth On Linings and Enclosure Smoke-Filling. *Journal of Fire Protection Engineering*, **8**, 183-193, 1996

6. Floyd, J., Hunt, S., Williams, F. and Tatem, P., A Network Fire Model for the Simulation of Fire Growth and Smoke Spread in Multiple Compartments with Complex Ventilation. *Journal of Fire Protection Engineering,* **15**, 199–229, 2005

7. Trouvé, A. and Wang, Y., Large eddy simulation of compartment fires, *International Journal of Computational Fluid Dynamics*, **24**, 449-466, 2010

8. Wahlqvist, J. and Van Hees, P., Validation of FDS for large-scale well-confined mechanically ventilated fire scenarios with emphasis on predicting ventilation system behavior. *Fire Safety Journal*, **62**, 102-114, 2013

9. Jenft, A., Collin, A., Boulet, P., Pianet, G., Breton, A. and Muller, A., Experimental and numerical study of pool fire suppression using water mist, *Fire Safety Journal Volume*, **67**, 1-12, 2014

10. Chow, W., Gao, Y., Zhao, J., Dang, J. and Chow, N., A study on tilted tunnel fire under natural ventilation. *Fire Safety Journal*, **8**, 44–57, 2016

11. Hsu, W., Huang, Y., Shen, T., Cheng, C., and Chen, T., Analysis of the Hsuehshan Tunnel Fire in Taiwan. *Tunnelling and Underground Space Technology*, **69**, 108–115, 2017

12. Li, Y., Fan, C., Ingason, H., Lönnermark, A. and Ji, J., Effect of cross section and ventilation on heat release rates in tunnel fires. *Tunnelling and Underground Space Technology*, **51**, 414–423,2016

13. Li, Y., and Ingason, H., Effect of cross section on critical velocity in longitudinally ventilated tunnel fires, *Fire Safety Journal*, **91**, 303–311, 2017

14. Haghighat, A., Luxbacher, K., and Lattimer, B., Development of a Methodology for Interface Boundary Selection in the Multiscale Road Tunnel Fire Simulations. *Fire Technology,* **54**, 1029–5066, 2018

15. Ang, C., Rein, G., Peiro, J., and Harrison, R., Simulating longitudinal ventilation flows in long tunnels: Comparison of full CFD and multi-scale modelling approaches in FDS6. *Tunnelling and Underground Space Technology*, **52**, 119–126, 2016

16. Vermesi, I., Rein, G., Colella, F., Valkvist, M., and Jomaas, G., Reducing the computational requirements for simulating tunnel fires by combining multiscale modelling and multiple processor calculation. *Tunnelling and Underground Space Technology*, **64**, 146–153, 2017.

17. Colella, F. (2010). Multiscale Modelling of Tunnel Ventilation Flows and Fires, Edinburgh, 2016

18. Colella, F., Rein, G., Borchiellini, R., and Torero, J., A Novel Multiscale Methodology for Simulating Tunnel Ventilation Flows During Fires. *Fire Technology*, **47**, 221–253, 2011

19. Colella, F., Rein, G., Verda, V., and Borchiellini, R., Multiscale modeling of transient flows from fire and ventilation in long tunnels. *Computers & Fluids*, **51**, 16–29, 2011

20. Colella F., Rein, G., Verda V., Borchiellini R. and Torero, J.L., Time-dependent Multiscale Simulations of Fire Emergencies in Longitudinally Ventilated Tunnels. *Fire Safety Science*, **10**, 359-372, 2011

21. Cosentino, S. Innovative Modelling Approaches For the Design, Operation and Control of Complex Energy Systems with Application to Underground Infrastructures. Torino. (2016)

22. Chandrashekar, M. and Wong, F., 1982. Thermodynamic system analysis – a graph-theoretic approach. *Energy*, **7**, 539-566, 1982

23. Sciacovelli, A., Verda, V. and Borchiellini, R., *Numerical Design of Thermal Systems.* Clut. 2013

24. Patankar, S., *Numerical Heat Transfer and Fluid Flow*. Tayor & Franci, 1980

25. Quarteroni, A., Valli A., *Domain Decomposition Methods for Partial Differential Equations*, Oxford Science Publications, 1999.

26. McGrattan, K., Hostikka, S., McDermott, R., Floyd, J. and Vanella, M., *Fire Dynamics Simulator Technical Reference, Guide: Volume 1: Mathematical Model.* NIST Special Publication 1018, 2013